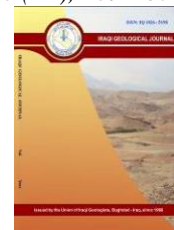




Iraqi Geological Journal

Journal homepage: <https://www.igi-iraq.org>



Using Passing Trains as Seismic Sources for Refraction Microtremor Site Characterisation Surveys: Rugeley, Staffordshire, UK

Raad Eissa^{1,2*}, Nigel Cassidy^{1,3}, David Gunn⁴, Ian Stimpson¹, Ben Dashwood⁴, Dave Morgan⁴, Jamie Pringle¹ and Jonathan Lee⁴

¹ School of Geography, Geology, and Environment, Faculty of Natural Sciences, William Smith Building, Keele University, Staffordshire, ST5 5BG, UK

² College of Engineering, Civil Engineering Department, University of Kerbala, Kerbala, Iraq

³ School of Engineering, University of Birmingham, Edgbaston, Birmingham, B15 2TT, UK

⁴ British Geological Survey, Keyworth, Nottingham, NG12 5GG, UK

* Correspondence: raad.m@uokerbala.edu.iq

Abstract

Received:
8 July 2022

Accepted:
21 October 2022

Published:
28 February 2023

Microtremor seismic surveys are routinely used to provide shear wave velocities that are converted to soil stiffness site profiles. In this paper, we look to assess the feasibility of using trains as seismic sources to characterize near-surface geology, define the optimum survey parameters to collect train-induced vibrations (i.e., array location and orientation to the railway) and find how the geology affects train-induced vibration characteristics. Three-component train-induced shear wave vibrations were recorded on short (44 m) and long (115 m) linear seismic arrays, both parallel and orthogonal to the nearby railway embankment, using standard seismic refraction recording equipment. The collected data were divided into short/long array size/orientation and seismic components for each survey configuration. 1D shear wave velocity-depth profiles were also generated for all data sets. Results showed that long linear arrays with vertical components, parallel to the railway embankment, was optimal with the greater depth ranges. The vertical component amplitude of train-induced vibrations was found to be affected by the site geology, increasing with the thickening of Quaternary deposits and having different magnitudes for trains traveling in different directions. Results showed that different apparent shear-wave velocities were obtained from different train groups and different seismic components. The passenger trains (i.e. Virgin Trains Pendolino and British Midland 319 series) generate Rayleigh waves at higher frequencies than the freight trains.

Keywords: Train-induced vibration; Rayleigh wave; Shear wave velocity; Site characterization

1. Introduction

For engineering and construction projects, detailed geotechnical site investigations are critical to obtaining physical and mechanical ground parameters. Traditionally, comprehensive drilling and trial pit campaigns are the most popular geotechnical investigative methods, in order to collect definitive samples from different depths below ground level for later testing (Reynolds, 2011). However, these are usually one-dimensional, site invasive, time-consuming, difficult to obtain in some sites and may not be representative on more heterogeneous sites, such as in urban areas where the geology is complex. Near-

surface geophysical investigations have the potential to provide site characterization and highlight problematic areas for subsequent geotechnical investigations (Reynolds, 2011; Foti et al., 2015).

Multichannel Analysis of Surface Waves (MASW) and Refraction Microtremor (ReMi) seismic surveys are being increasingly used for site characterization. They are usually quick and relatively cheap to collect, and results can be viewed in the field (Mathews et al., 1996). Mathews et al. (1996) showed how seismic data generated from active sources (e.g. vibrator, sledgehammer source) could determine soil stiffness-depth profiles, a critical component of geotechnical site investigations. Seismic shear wave velocities are related to Rayleigh wave velocities, and the shear modulus can be obtained from this by using the following equations:

$$V_S = V_{P_R} \quad (1)$$

$$G = \rho V_S^2 \quad (2)$$

Where V_S is shear wave velocity, P is a function of Poisson's ratio, V_R is Rayleigh wave velocity, G is shear modulus, and ρ is soil bulk density.

The corresponding depth to a shear wave velocity estimate is a function of the Rayleigh wave wavelength. Consequently, the frequency range of the Rayleigh waves recorded determines the upper and lower depths for which shear wave velocity determinations are valid.

More recently, passive source ReMi surveys are being undertaken (see, for example, Foti et al., 2015), utilizing natural sources, for example, wind (see, e.g. Gassenmeier et al., 2015), anthropogenic sources (mechanized transport) (Behm et al., 2014) or indeed combining with active seismic surveys (Yalcinkaya et al., 2016). Train-induced vibrations are potentially problematic along railway routes (Gunn et al., 2015; Krylov, 2015; Fu, 2016), but they can be useful as seismic sources for seismic surveys for site characterisation. The pressure of the train wheel-axles causes each sleeper to act as a source of seismic energy, creating a displacement field that moves along with the train (Gunn et al., 2015). Kouroussis et al. (2014) state that Rayleigh waves are the chief component of train-induced vibrations compared to P and S-waves. There has been some modeling work undertaken to study critical velocity of waves produced from passing trains (Krylov, 1995; Ju and Lin, 2004) and the Rayleigh wave generation (Ju et al., 2010), but not their use as a seismic source.

Nakata et al. (2011) record train vibrations and apply the cross-coherence method using seismic interferometry to recover body and surface waves. A transverse component of the retrieved surface waves (Love waves) was used as a demonstration to determine shear wave velocity-depth profile down to about 300m. Quiros et al. (2016) recorded the vertical component of train-induced vibrations using a 25m geophone spacing, 2,475 m total length linear array. The collected data were processed using seismic interferometry to retrieve body and surface waves (Rayleigh waves). They found moving trains can generate surface waves containing frequencies in the range of 1-14 Hz and a shear wave velocity-depth profile was determined through an inversion process using dispersion curves down to about 180 m for the studied site. Furthermore, Liu et al. (2021), performed seismic interferometry method to retrieve surface seismic waves from train-induced vibrations. They found that the surface waves could be utilized for near surface investigations.

Nakata et al. (2011), Quiros et al. (2016), Fuchs et al. (2017) and Liu et al. (2021) state that the moving trains can be a good seismic source for surface wave studies, can be used to estimate shear wave velocity for shallow depths and utilised for a range of applications such as site investigation.

This study assesses the feasibility of using trains as seismic sources to characterize near-surface geology, to define the optimum survey parameters to collect train-induced vibrations (i.e., array location and orientation to the railway), and to find how the geology affects train-induced vibration characteristics. The study collects a series of ReMi seismic survey datasets using different sized linear arrays with different orientations to the railway. Three component-ground motion are recorded; vertical, horizontally parallel to the railway (HP), and horizontal orthogonal to the railway (HO), and results from

different seismic components, and different train directions (SE-bound and NW-bound trains) will be compared.

2. Site Characterisation

The study site was adjacent to the “West Coast Main Line” rail-line in the UK between the towns of Rugeley and Lichfield in Staffordshire (Fig. 1). This is a busy transport route, with a mixture of passenger and freight trains using the railway. There are low hills to the north, but the site on the River Trent Valley flood plain is generally flat and the water table is generally about 8 m below ground level.

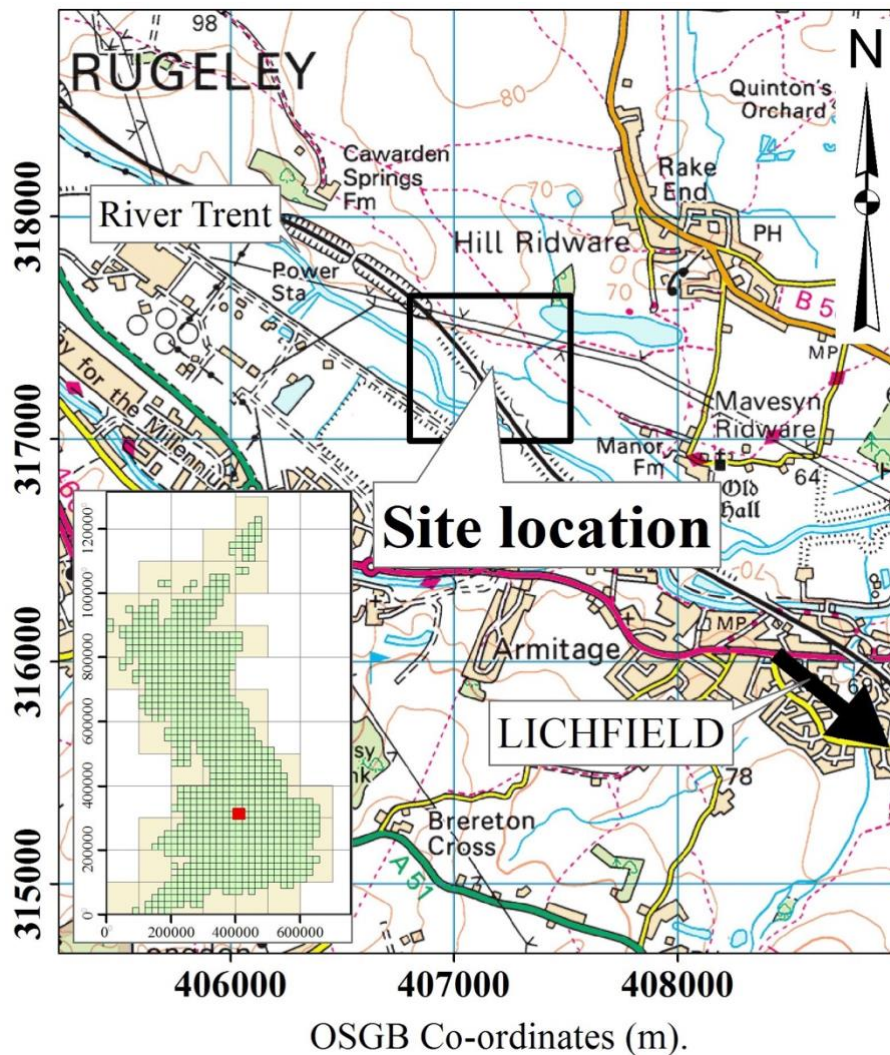


Fig. 1. Site map (with location map inset) showing the train line and location. The black line in NW-SE direction shows the railway route. Basemaps are © Crown Copyright/Database Right 2016, an Ordnance Survey/EDINA Supplied Service.

Nearby borehole records (BGS Geindex, 2018) indicate that the bedrock is composed of the Triassic Chester and Helsby Sandstone Formations, consisting of brown, red and grey interbedded pebbly sandstones, siltstones, and mudstones. Overlying these are Quaternary deposits linked to the River Trent. Towards the end of the last glaciation meltwater over-deepened the river valley which was then backfilled with glacial outwash sediments. These are topped by post-glacial and recent river terrace and alluvium deposits from the River Trent (Fig. 2). The railway runs northeast of the deepest part of the river channel.

The train line, built in the middle of the 19th century (Clark, 1967), is electrified for higher speed trains (although diesel engines also use the line) and is on a raised earthen embankment running northwest-southeast (Fig. 2) across the site. The embankment height decreases northward and enters a cutting beyond the site in order to maintain the track 'at grade'. The studied site is close to the HS2 (High Speed 2) proposed route. Therefore, this work has implications for ground surveys for the HS2 both here and elsewhere.

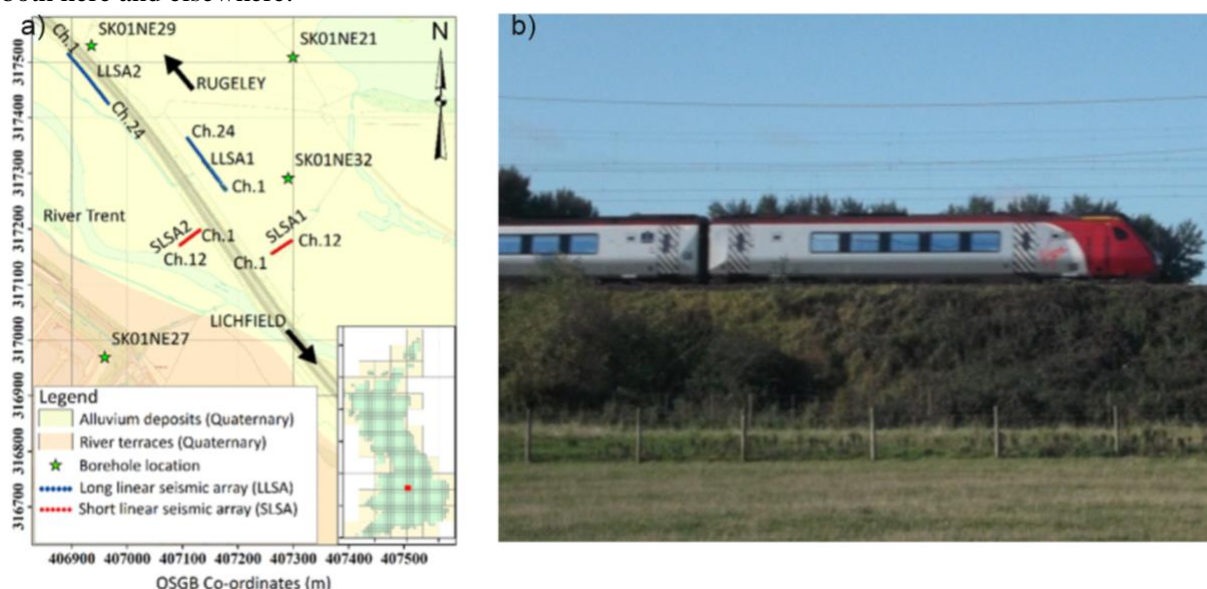


Fig. 2. a) Superficial deposit (alluvium and river terrace) distribution (BGS DiGMapGB-10, 2018) at the studied site (with location map inset), boreholes locations, and field deployment of the seismic arrays used for data acquisition. The grey lines trending NW-SE show the railway tracks. Basemaps are © Crown Copyright/Database Right 2016, an Ordnance Survey/EDINA Supplied Service, b) site photograph showing the raised railway embankment. Photograph direction is southwest.

3. Data Acquisition

Data were collected using three-component 4.5 Hz seismic geophones, and two different array lengths with different geophone spacings and different orientations relative to the railway, to determine optimal array configurations (Table 1). A Geode Seismograph, linked to a laptop computer running Seismodule controller software (Geometrics) was utilized to collect the vertical seismic component data whilst an ABEM Terraloc seismic system was used to collect the two horizontal seismic components.

Table 1. Seismic array configurations used for data acquisition. The distances for short linear arrays are measured for the first seismic station only, for the long arrays the distances are for all seismic stations (i.e. all the array).

Array type	No. of seismic stations	Station spacing (m)	Total array length	Orientation to railway embankment	Distance from railway embankment (m)
SLSA1	12	4	44	Orthogonal	30 east
SLSA2	12	4	44	Orthogonal	6 west
LLSA1	24	5	115	Parallel	30 east
LLSA2	24	5	115	Parallel	6 west

Data were collected from different passing train types, including passenger trains from the 319 Series London Midland (4-carriage) and Virgin Pendolino (9- or 11-carriage) trains, as well as freight trains (about 30 wagons), traveling in both directions, to discover if there were any directional effects.

Seismic arrays were designated "short" and "long" Linear Seismic Arrays (LLSA and SLSA) depending upon the total array length (summarized in Table 1). Finally, the seismic arrays were also undertaken at both 6 m (on west side) and 30 m (on east side) from the railway embankment. Data were collected with a 2 ms sample interval and a 32s record duration for each passing train.

4. Data Processing

The data were processed using ReflexW™ v.8.1 (Sandmeier geophysical research) software, then further separated into subsets for trains traveling SE and NW (SE-bound and NW-bound trains). ReflexW™ software was used to plot particle motion diagrams to investigate if the vibrations recorded were consistent with Rayleigh waves (Fig. 3). Other particle motion plots were prepared using MatLab software code to determine the nature (i.e., prograde or retrograde) of the wave propagation.

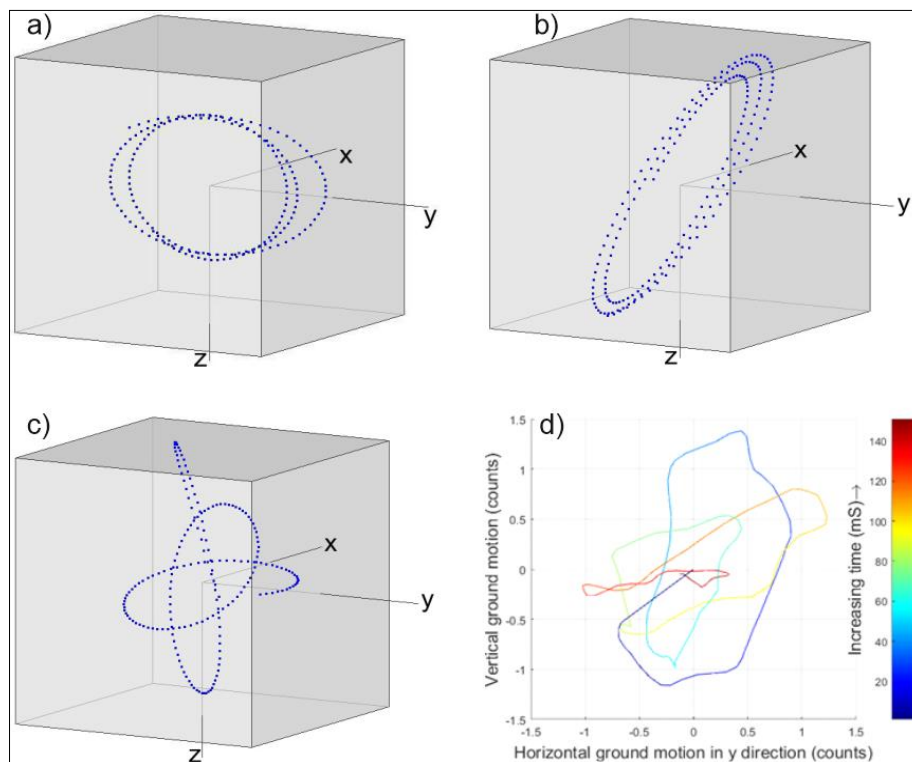


Fig. 3. Particle motion plots: (a) NW-bound London Midland passenger train; (b) NW-bound Virgin Pendolino and (c) SE-bound freight train. The x axis is parallel to the railway embankment and y axis is orthogonal; 300 samples (i.e. 0.6 second), d) Particle motion plot of NW-bound Pendolino, yz view; 150 samples (i.e. 0.3 second).

The subsets were then imported into SeisImager™/SW (version 5.2.1.3, Geometrics / OYO). The SeisImager/SW consists of two modules: Pickwin™ and WaveEq™. The Pickwin™ is used for generating dispersion curves using the Spatial Autocorrelation method (SPAC), and WaveEq™ is used to invert the dispersion curve and produce 1D shear-wave velocity-depth profiles via a non-linear least square inversion algorithm. These profiles are routinely used for site investigations.

5. Results and discussion

5.1. Comparison of Seismic Surveys from Passing Trains Travelling in Different Directions

5.1.1 Comparison of the effective investigated depth range

The datasets from the three seismic components were processed to produce 1D shear-wave velocity-depth profiles that were processed using all trains, both SE-bound and NW-bound trains. Generally, the long straight seismic arrays (LLSA1 and LLSA2) datasets for all the trains had a greater range of effective investigated depth than the short arrays, as would be expected (Fig. 4, 5 and 6 for the LLSA1 dataset examples. The differences in the investigated depth between the long and short arrays are related to the length of the deployed arrays. The longer array the deeper investigated depth and, therefore, the investigated depth of the long arrays cannot be compared with the investigated depth of the short arrays.

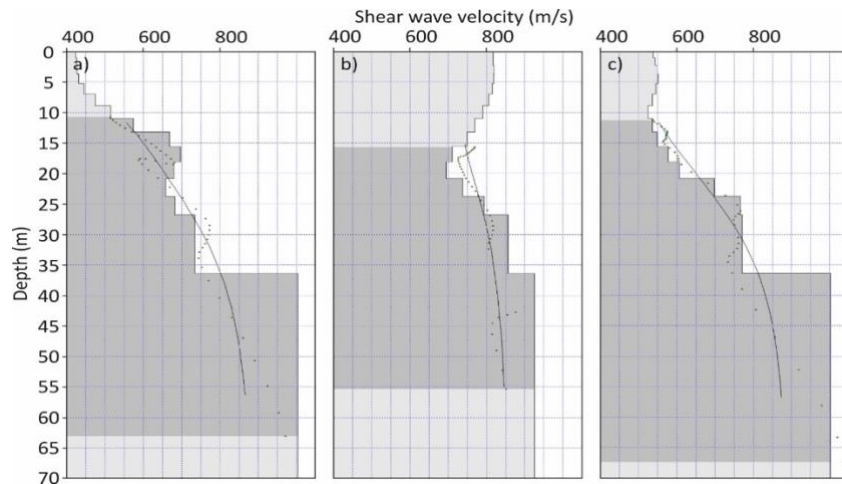


Fig. 4. Shear-wave velocity-depth profile from vertical component data acquired from LLSA1, a) for all trains, b) for SE-bound trains, and c) for NW-bound trains. Dots on profiles show results generated using one third wavelength method; the curve on the profile represents the theoretical dispersion curve. The dark grey area shows the effective investigated depth.

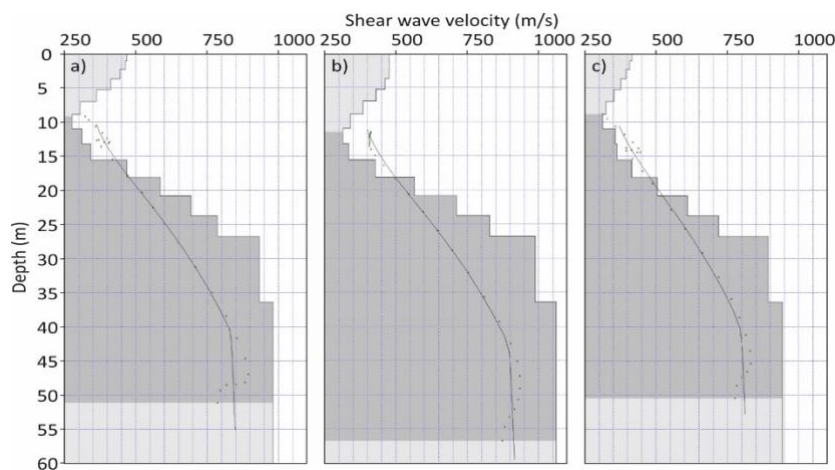


Fig. 5. Shear-wave velocity-depth profile from horizontal component parallel to the railway embankment, data acquired from the LLSA1, a) for all trains, b) for SE-bound trains, and c) for NW-bound trains. Dots on the profile show results generated using one third wavelength method; the curve on the profile represents the theoretical dispersion curve. The dark grey area shows the effective investigated depth.

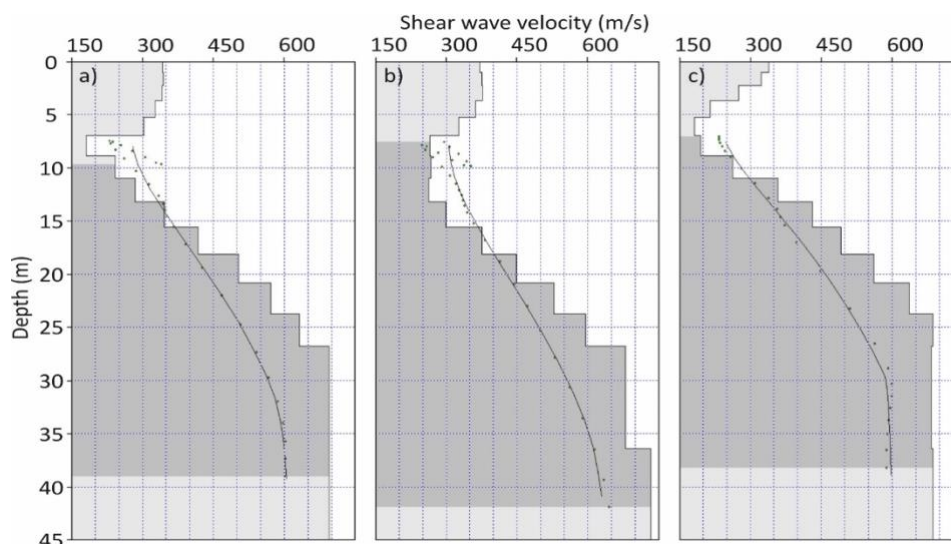


Fig. 6. Shear-wave velocity-depth profile from the horizontal component orthogonal to the railway embankment, data acquired from the LLSA1, a) for all trains, b) for SE-bound trains, and c) for NW-bound trains. Dots on the profile show results generated using one third wavelength method; the curve on the profile represents the theoretical dispersion curve. The dark grey area shows the effective investigated depth.

The comparison would mainly be among the investigated depths from different seismic components of the same seismic array. The short linear seismic arrays typically gave results that were not consistent with known ground conditions; see Fig. 7. The valid depth range of shear-wave velocities for all the collected data sets of the long and short linear arrays are summarized in

Table 2.

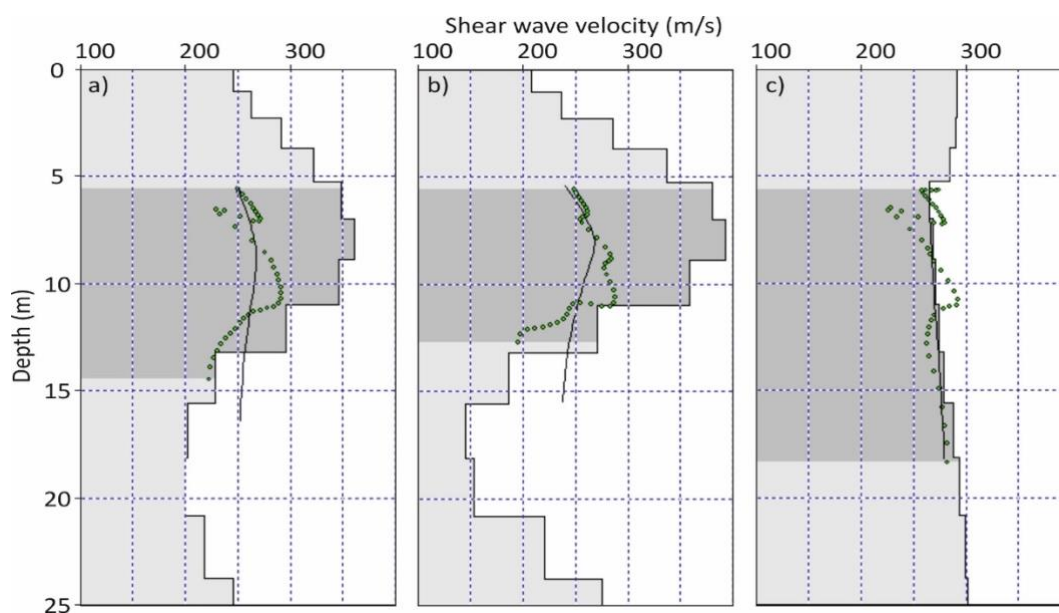


Fig. 7. Shear-wave velocity-depth profile from the vertical component, data acquired from the SLSA1, a) for all trains, b) for SE-bound trains, and c) for NW-bound trains. Dots on the profile show results generated using one third wavelength method; the curve on the profile represents the theoretical dispersion curve. The dark grey area shows the effective investigated depth.

Table 2. Depth range bgl of valid shear-wave velocity determinations for all the collected data sets, depths measured in metres; V is the vertical component, HP is the horizontal parallel component and HO is the horizontal orthogonal component.

Array	All trains group			NW-bound trains			SE-bound trains		
	V	HP	HO	V	HP	HO	V	HP	HO
LLSA1	10-60	8-50	8-40	10-65	10-50	8-38	15-55	10-55	7-40
LLSA2	10-50	8-35	7-30	10-50	10-35	7-30	10-50	10-40	7-30
SLSA1	6-14	6-14	5-17	6-18	7-13	7-18	6-13	6-15	6-17
SLSA2	6-22	7-16	6-17	6-22	11-15	6-16	7-22	7-16	6-16

The investigated depth bgl ranges for the vertical component of datasets recorded from the LLSA1 and LLSA2 were greater than the investigated depth range bgl for the horizontal components (

Table 2). For all the datasets, the horizontal parallel component resolved velocities deeper than the horizontal orthogonal component. This confirms that low frequency Rayleigh waves are best recorded on vertical component geophones, and they are better recorded as coherent waves as the train is approaching or receding the geophone array on the horizontal parallel component than on the horizontal orthogonal component when the train is adjacent to the array as the Rayleigh waves are less incoherent. There was little observable difference between SE-bound and NW-bound trains datasets.

5.1.2 Comparison of shear-wave velocity profiles

Because the long linear seismic arrays resulted in deeper effective investigated depths bgl, the resulting shear wave velocity-depth profiles from the arrays will be used to compare wave velocities from different seismic components and different train groups.

The vertical component data produce different shear-wave velocity-depth profiles from different train directions, e.g., see the LLSA1 datasets (Fig. 8 and 9). The horizontal components (both HP and HO) show good agreement between velocities obtained from the three directions for train groups. However, the velocities determined at a particular depth were lower for the HO component than they were for HP, and neither particularly matched the velocity profiles from the vertical component (Fig. 8).

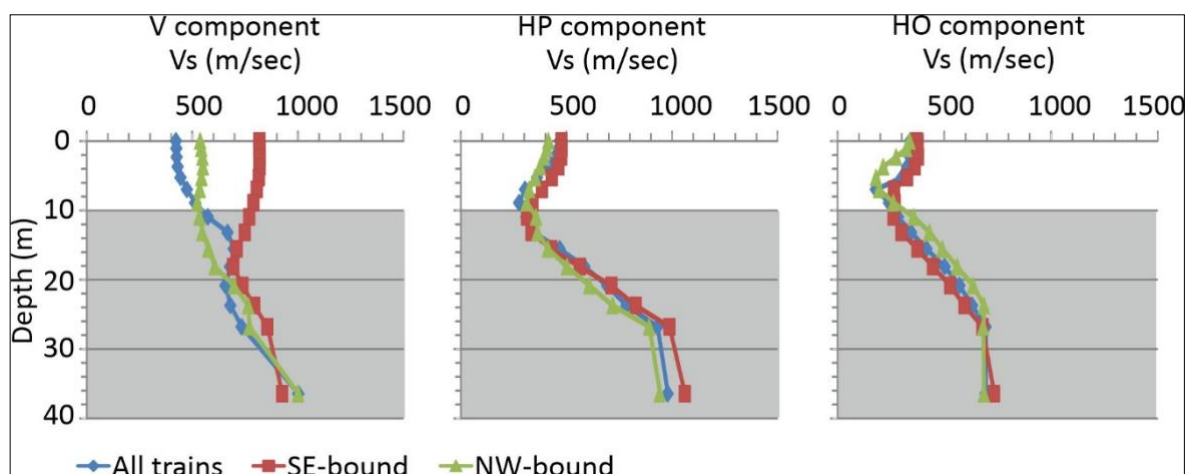


Fig. 8. Shear wave velocity comparison based on the seismic components using data from the LLSA1, showing the three components and using data from all passing trains. The dark grey area shows the effective investigated depth.

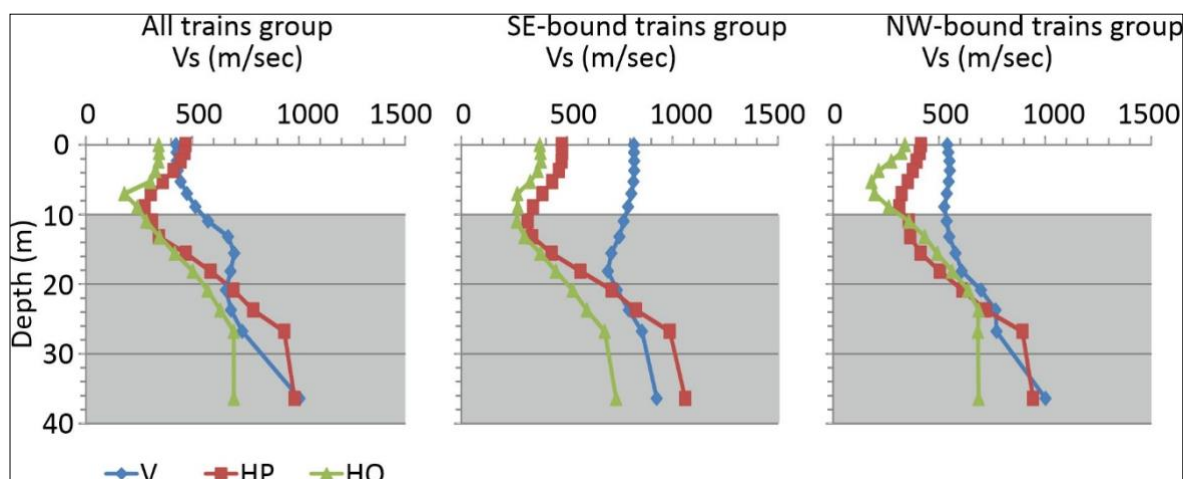


Fig. 9. Shear wave velocity comparisons based on the train groups using data from the LLSA1, showing three components and using data from all passing trains. The dark grey area shows the effective investigated depth.

Comparison of the shear-wave velocity-depth profiles, on different seismic components and different trains groups, from data recorded from the LLSA2 array had almost the same results as from the LLSA1, see Fig. 10 and Fig. 11.

To check the different apparent wave velocities, on different seismic components, frequency-wavenumber analysis was carried out; 1) to check if apparent wave velocities were recorded by comparing the positive part of the f-k transform with the negative part of the f-k transform, and 2) to inspect if refracted body waves were observed alongside with observed surface waves, as this analysis was applied in previous studies, see, for example, Quiros et al. (2016).

The frequency-wavenumber (f-k) analysis of raw recorded vibrations generated by Pendolino passenger trains traveling either destination (i.e., SE-bound and NW-bound trains) and from vertical, horizontal parallel, and horizontal orthogonal components was carried out for the different train positions (i.e., trains approaching, adjacent and receding). Due to the short recording time (32 seconds for the whole seismic record) and due to the even smaller recording time window for the approaching, adjacent, and receding parts, the f-k analysis was not informative enough to deliver a robust interpretation. Fig. 12 shows the f-k analysis for a SE-bound Pendolino passenger train and when the train approached the site, the recording time window was 4 seconds.

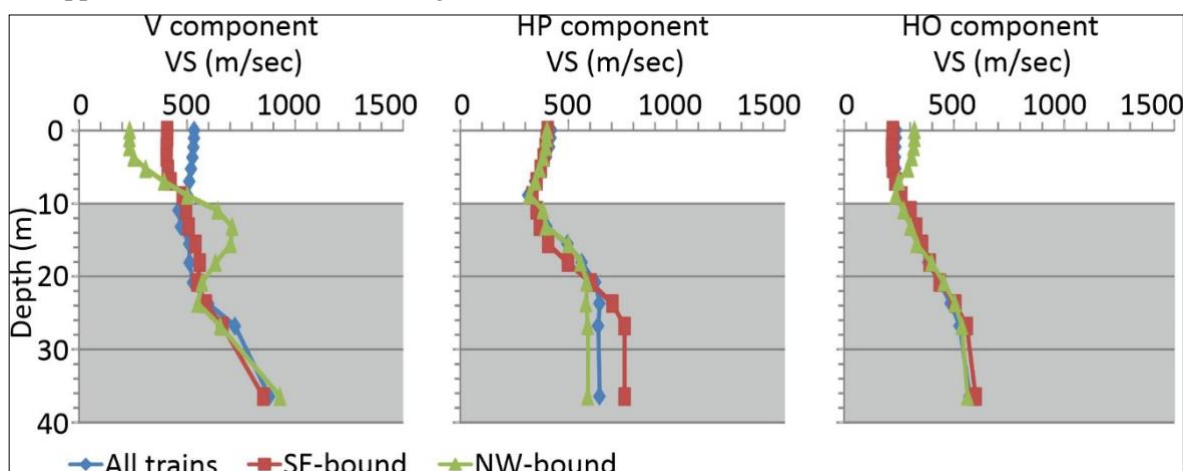


Fig. 10. Shear wave velocity comparisons based on the seismic components using the data from the LLSA2, showing three components and using data from all passing trains. The dark grey area shows the effective investigated depth.

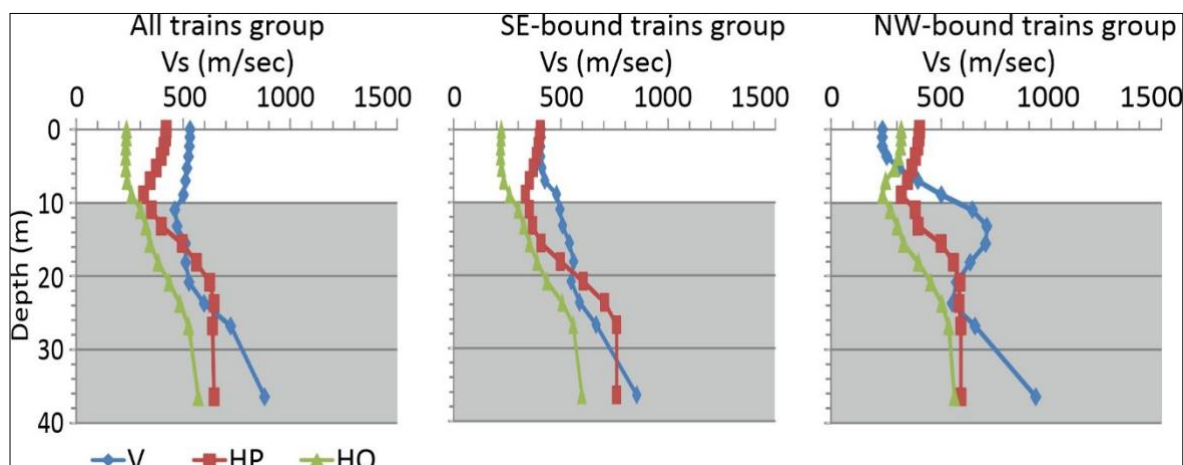


Fig. 11. Shear-wave velocity comparisons based on the train groups using the data from the LLSA2, showing three components and using data from all passing trains. The dark grey area shows the effective investigated depth.

The asymmetry between the positive and the negative parts of the f - k transform indicates to the apparent wave velocity was recorded. When the train is adjacent to the seismic array, most of the generated vibrations are approaching broadside the array, which means, as long as the train is parallel to the array, an infinite wave velocity might be recorded. On the f - k transform, when the train receding, the propagated energy appears more on the negative part of the transform, which indicates for recording apparent wave velocity.

Another possible reason for the different shear wave velocities on different seismic components might be, related to the site's heterogeneity and observing Love waves on the horizontal components and Rayleigh waves on the vertical component. Safani et al. (2005) found different shear wave velocities at the same investigated depth, from inverting Rayleigh and Love wavefields collected at the same site and time. At 17 m depth, shear wave velocity calculated using Rayleigh wave was found to nearly double of that calculated using Love waves. The variations of the measured shear wave velocity were interpreted due to the site anisotropy.

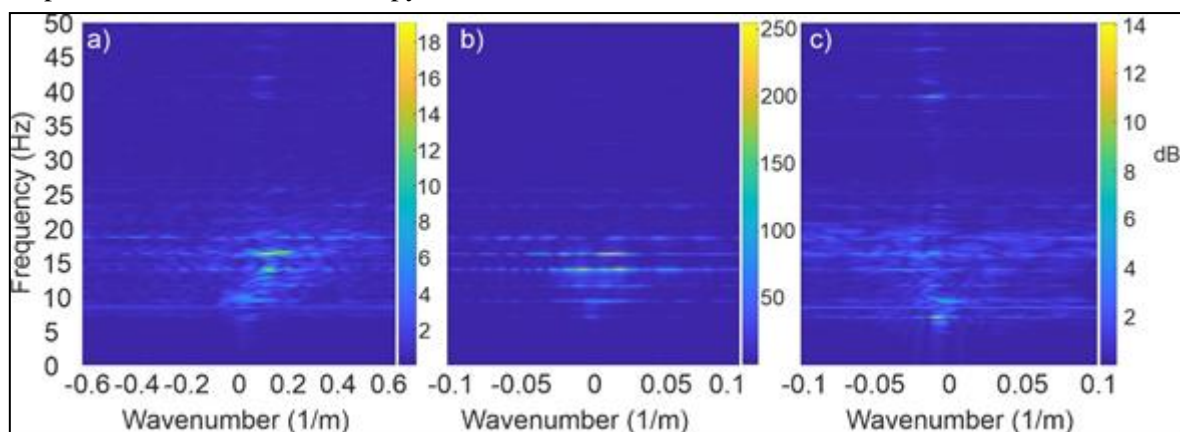


Fig. 12. f - k analysis for a SE-bound Pendolino passenger train, a) when the train is approaching the array, b) when the train is adjacent to the array and c) when the train is receding the array. Data used was collected at LLSA 1. The time window here is 4 seconds.

Vibrations from a moving train can be generated by two different vertical and horizontal excitation mechanisms; the vertical vibrations are produced by the vertical loading of the underlying physical sleepers under the railway track, whereas horizontal vibrations may come from train wheel-railway track

interactions (Li et al., 2017). Song et al. (1989) state that Love wave can be observed using horizontal geophones oriented orthogonal to the array length, which is similar to the horizontal orthogonal component (HO) in this study. Ultimately, the observed vibrations on the horizontal parallel (HP) and horizontal orthogonal (HO) components can be more consistent with Love waves rather than Rayleigh waves. Because the moving trains, as a seismic source, kept moving during the recording time and the seismic array deployed at a side of the railway (i.e. the seismic source is not in line with the array), therefore, not one of the three deployed seismic components can be totally consistent with the generated vibrations and it might be that the seismic components have different sensitivity to the generated Love and Rayleigh waves during recording time (Fig. 13) and (Table 3).

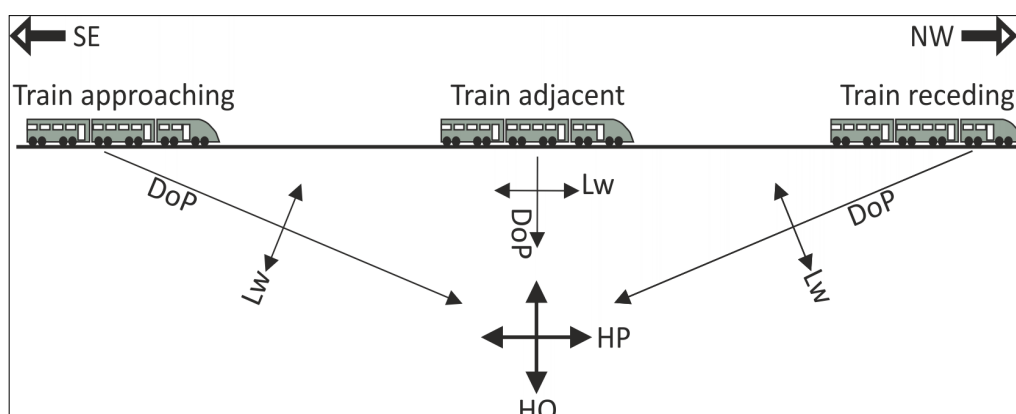


Fig. 13. Schematic diagram shows how the generated Love wave approaches the horizontal parallel (HP) and the horizontal orthogonal (HO) components when the train approaching, adjacent, and receding, DoP is the Direction of Propagation and Lw is the Love wave.

Table 3. The three seismic components compatibility with generated Love and Rayleigh waves during recording time. Wave type in parentheses indicates to less response between that certain wave type and that seismic component.

Train position	Vertical component	Horizontal component	parallel	Horizontal component	orthogonal
Train approaching	Rayleigh	Rayleigh (Love)		Love (Rayleigh)	
Train adjacent	Rayleigh	Love (Rayleigh)		Rayleigh (Love)	
Train receding	Rayleigh	Rayleigh (Love)		Love (Rayleigh)	

Based on this analysis, in this study, if the difference in shear wave velocities between the horizontal parallel and the horizontal orthogonal components are ignored, the difference between the wave velocity on the vertical component (i.e., inverting Rayleigh wave) and the wave velocity on the horizontal components (i.e., inverting Love wave) might be related to the site's heterogeneity.

Other studies have also shown that the railway embankment has noticeable effects on the vibrations, for example, the frequency range and the waveguide effects (Ditzel and Herman, 2004; Connolly et al., 2013). The embankment's waveguide effect may also help generate variations in shear wave velocities from different seismic components.

5.2 Particle Displacement on the Vertical Seismic Component

The maximum and minimum amplitudes of the vertical component were measured on all 24 geophones for LLSA1, all being at a distance of 30 m from the embankment, with channel 1 at the southeast end of the array (Fig. 2).

Fig. 14 shows that the maximum and minimum values on the vertical component from NW-bound trains are smaller than those for SE-bound trains even when the shorter distance from the array to the NW-bound train track is taken into account. This is also true for array SLSA2, even though SE-bound trains use the farthest rail track from that array. In addition, the maximum value of the vertical component for SE-bound trains increased towards the southeast, whilst for NW-bound trains, the maximum value of the vertical component remained fairly constant across the array. This can only be interpreted as being due to an effect of the thickness variation of superficial deposits, which increases towards the southeast.

5.3. Comparison of Rayleigh Wave Content from different Trains

The particle motion plots for different trains (i.e., Pendolino, 319 Series and Freight trains) represented in Fig. 3 show different complexity. Passenger trains produce vibrations that are more consistent with a simple Rayleigh wave source than those of freight trains. When passenger trains are approaching and receding from the site, they effectively act as point sources, only behaving as complex multiple sources for each axle as the train is adjacent to the array. The freight trains being longer, and with a lower dominant frequency, behave as a complex multiple sources for a greater range of distances.

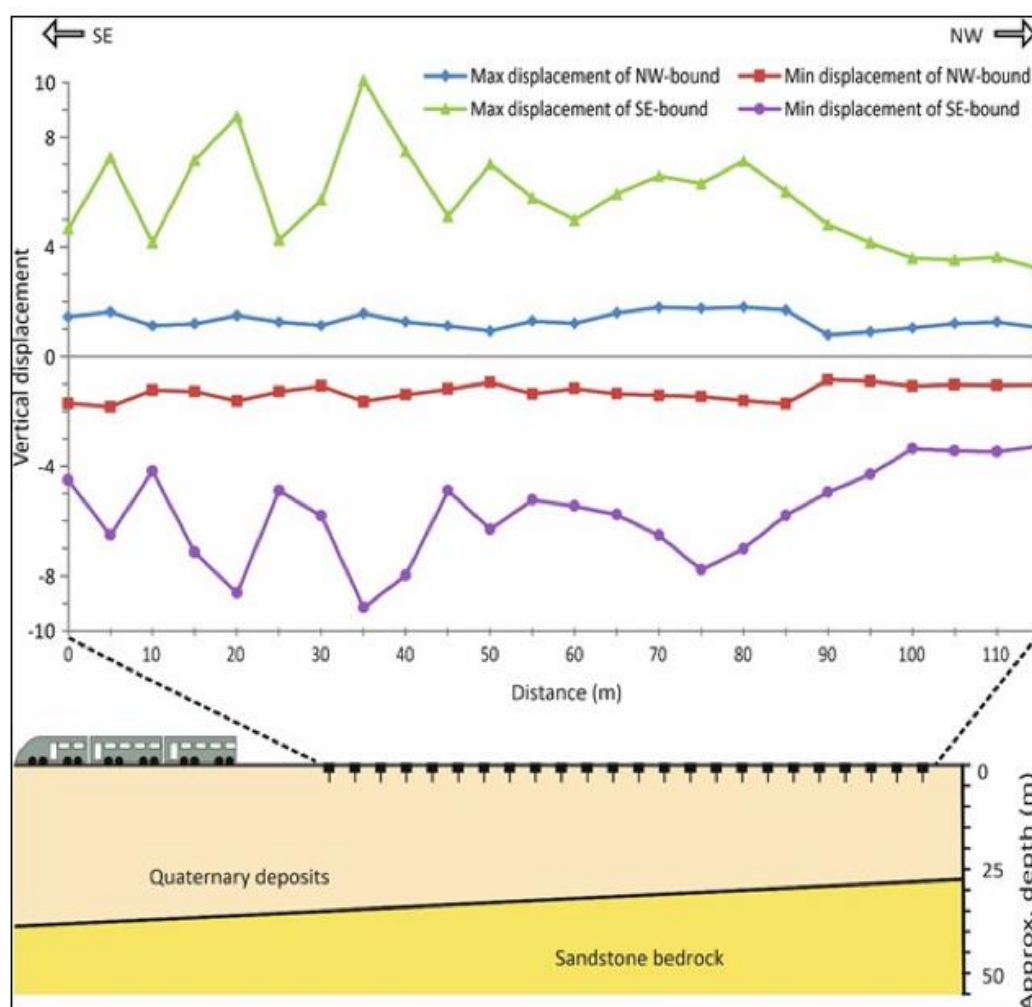


Fig. 14. Maximum and minimum vertical particle displacement when passenger train (Pendolino) passing the site in either direction. Displacement values represented in the figure are averaged for three passing trains (i.e. records). Geophones were spaced 5 m apart.

6. Conclusions

Particle motion plots show that the observed vibrations are consistent with Rayleigh waves. The vertical component amplitude of NW-bound trains is smaller than those of SE-bound trains. The vertical component of the SE-bound trains was found to increase to the SE, whilst for the NW-bound trains was found to be fairly constant. This was interpreted to be due to the inclined deposits-bedrock interface and to the increase in the thickness of the deposits to the SE.

The vibrations observed by the linear seismic arrays, oriented parallel to the railway line, produced more valuable shear wave velocity-depth profiles (i.e., covered wider effective investigated depth and increasing in shear wave velocity with depth) than those generated from linear seismic arrays oriented orthogonal to the railway.

The resolved shear wave velocity-depth profiles from different seismic components showed different shear wave velocities with depth. The vertical component resolved the largest wave velocity, whilst the horizontal component orthogonal to the railway component resolved the smallest wave velocity, which cannot be the case for the same piece of ground. The differences in the resolved wave velocities were interpreted due to the poor alignment between the deployed array and the seismic source (the trains). Therefore, most of the generated vibrations will be approaching the arrays obliquely and/or broadside and apparent wave velocities were observed rather than true wave velocities. This interpretation can be confirmed by the frequency-wavenumber analysis.

Another possible interpretation might be due to observing the Rayleigh wave on the vertical component and the Love wave on the horizontal components. Inverting Love wave and Rayleigh wave using the same software package (the SeisImager/SW) which has no certain option to process Rayleigh wave differently from Love wave.

Acknowledgements

The British Geological Survey are thanked for facilitating site access, providing logistical support and technical advice. A 2003 SRIF2 UK Research Council award supported the geophysical equipment used during this research. EDINA Digimap is acknowledged for data retrieval support. James Francis, Nicholas Cooper, Joe Ainsworth, Nick Mason and Cathrene Rowell (all Keele University) are thanked for field and logistical assistance.

References

- Behm, M., Leahy, G.M., Snieder, R., 2014. Retrieval of local surface wave velocities from traffic noise – an example from the La Barge basin (Wyoming). *Geophysical Prospecting*, 62, 223-243.
- Clark, P.L., 1967. 'Railways' in M. W. Greenslade and J. G. Jenkins (eds.) *A history of the county of Stafford volume II*. Oxford University Press (London).
- Connolly, D., Giannopoulos, A., Frode, M.C., 2013. Numerical modelling of ground borne vibration from high speed rail lines on embankment. *Soil Dynamics and Earthquake Engineering*, 46, 13-19.
- Ditzel, A., Herman, G.C., 2004. The influence of a rail embankment on the vibrations generated by moving trains. *Journal of Sound and Vibration*, 271, 937-957.
- Foti, S., Lai, C.G., Rix, G.J., Strobbia, C., 2015. *Surface Wave Methods for Near Surface Site Characterization*. CRC press, 467.
- Fu, C. 2016. Dynamic behaviour of a simply supported bridge with a switching crack subjected to seismic excitations and moving trains. *Engineering Structures*, 110, 59-69.
- Fuchs, F., Bokelmann, G., the AlpArray working group. 2018. Equidistant spectral lines in train vibrations. *Seismological Research Letters*, 89 (1), 56-66.
- Gassenmeier, M., Sens-Schonfelder, C., Delatre, M., Korn, M., 2015. Monitoring of environmental influences on seismic velocity at the geological storage site for CO₂ in Kertzin (Germany) with ambient seismic noise. *Geophysical Journal International*, 200, 524-533.

- Gunn, D., Williams, G., Kessler, H., Thorpe, S., 2015. Rayleigh wave propagation assessment for transport corridors. *Proceedings of the Institution of Civil Engineers – Transport*, 168, 487-498.
- Ju, S., Lin, H., 2004. Analysis of train-induced vibrations and vibration reduction schemes above and below critical Rayleigh speeds by finite element method. *Soil Dynamics and Earthquake Engineering*, 24, 993-1002.
- Ju, S.H., Liao, J.R., Ye, Y.L., 2010. Behaviour of ground vibration induced by trains moving on embankments with rail roughness. *Soil Dynamics and Earthquake Engineering*, 30, 1237-1249.
- Kouroussis, G., Connolly, D.P., Verlinden, O., 2014. Railway-induced ground vibrations: A review of vehicle effects. *International Journal of Rail Transportation*, 2(2), 69-110.
- Krylov, V.V., 1995. Generation of ground vibrations by superfast trains. *Applied Acoustic*, 44, 179-164.
- Krylov, V.V., 2015. Focusing of Rayleigh waves generated by high-speed trains under the conditions of ground vibration boom, 1-15.
- Li, P., Ling, X., Zhang, F., Li, Y., Zhao Y., 2017. Field testing and analysis of embankment vibrations induced by heavy haul trains. *Shocks and Vibrations*, 2017, 7410836.
- Liu, Y., Yue, Y., Li, Y., Luo, Y., 2021. On the retrievability of seismic waves from high-speed-train-induced vibrations using seismic interferometry. *IEEE Geoscience Remote Sensing*.
- Mathews, M.C., Hope, V.S., Clayton, C.R.I., 1996. The use of surface waves in the determination of ground stiffness profiles. In: *Proceeding of ICE - Geotechnical Engineering*. 119 (2), 84-95.
- Nakata, N., Snieder, R., Tsuji, T., Larner, K., Matsouka, T., 2011. Shear wave imaging from traffic noise using seismic interferometry by cross-coherence. *Geophysics*, 76(6), SA97-SA106.
- Quiros, D.A, Brown, L.D, Kim, D., 2016. Seismic interferometry of railroad induced ground motions: body and surface wave imaging. *Geophysical Journal International*, 205, 301-313.
- Safari, J., O'Neill, A., Matsuoka, T., Sanada, Y., 2005. Applications of love wave dispersion for improved shear-wave velocity imaging. *Journal of Environmental and Engineering Geophysics*, 10(2), 135-150.
- Song, Y.Y., Castagna, J.P., Black, R.A., Knapp, R.W., 1989. Sensitivity of near-surface shear-wave velocity determination from Rayleigh and Love waves. Expanded abstract of the 59th Annual meeting of the Society of Exploration Geophysicists, Dallas, Texas, 509-512.
- Yalcinkaya, E., Alp, H., Ozel, O., Gorgun, E., Martino, S., Lenti, L., Bourdeau, C., Bigarre, P., Coccia, S., 2016. Near-surface geophysical methods for investigating the Buyukcekeme landslide in Istanbul, Turkey. *Journal of Applied Geophysics*, 134, 23-35.